

Received July 20, 2019, accepted August 6, 2019, date of publication August 15, 2019, date of current version September 4, 2019.

Digital Object Identifier 10.1109/ACCESS.2019.2935534

# A Tradeoff Approach for Optimal Fault Detection of Networked Control Systems With Event-Triggered Scheme

ZHEN ZHAO<sup>1</sup>, JINFENG GAO, AND CHUNPING WANG

Faculty of Mechanical Engineering and Automation, Zhejiang Sci-Tech University, Hangzhou 310018, China

Corresponding author: Jinfeng Gao (gaojf163@163.com)

This work was supported by the National Natural Science Foundation of China under Grant 61374083.

**ABSTRACT** An optimal fault detection (FD) approach for a class of networked control systems (NCSs) is concerned in this work. To improve the accuracy of the FD, a new event-triggered scheme (ETS) is addressed, where the output measurement transmitted or not is determined by a set of conditions instead of a single condition. Moreover, output measurements in these conditions are not only the last transmitted data, but also the data in the past period of time. The structure of fault detection and isolation (FDI) consisting of the residual generation and residual evaluation can detect faults as accurately as possible, and show robustness to disturbances in the meantime. Optimal observer gains can be obtained by utilizing the discrete-time Riccati equation (DTRE), and the time-varying threshold can be specified by employing the linear matrix inequality (LMI). Finally, a numerical simulation and the application on closed-loop continuous stirred-tank reactor (CSTR) are adopted to prove the superiority of the proposed approach.

**INDEX TERMS** Networked control systems, event-triggered scheme, optimal fault detection, tradeoff, residual generation.

## I. INTRODUCTION

Networked control systems (NCSs), which transmit and exchange data over the communication network, have received much attention in recent decades. Comparing with traditional control systems, NCSs achieve remote control and resource sharing easily due to the shared communication networks [1], [2]. Furthermore, the difficulty and cost of equipment installation and maintenance are greatly reduced. Due to the advantages mentioned above, NCSs play a significant role in various fields, such as offshore structures [3] and unmanned aircraft vehicles (UAVs) [4].

To guarantee the control performance in a certain extent, NCSs adopt a periodic sampling scheme, namely time-triggered scheme. However, it will release a large amount of redundant data, occupy the networked bandwidth heavily, and brings about poor quality of service (QoS). The event-triggered scheme (ETS) proposed in late 1990s is an effective solution, in which transferring task is only carried out after the well-designed event occurs. The scheme can significantly alleviate the resource

occupation while ensuring satisfactory performance so that it is applied to many control systems, such as fuzzy control systems [5], [6], multi-agent systems (MAS) [7]–[9] and so on. In ETS-related research, many achievements have been obtained, which basically can be made into three classifications according to literature [10], namely, event-triggered sampling scheme (ETSS) [11], [12]; self-triggered sampling scheme (STSS) [13]–[15]; and discrete event-triggered communication scheme (DECS) [7], [16]. ETS with multiple quantization is put forward in [17], [18] to further reduce the communication burden. The authors in [19] overcome the drawback which controller cannot be co-designed with ETS, and the co-design strategy also has a nice application in fuzzy systems with asynchronous constraints in [20]. To ensure the MAS can converge under any initial conditions, the authors propose the fixed-time event-triggered control (ETC) in [21]. For acquiring a suitable threshold, ETS with adaptive thresholds is addressed in [22]. To reduce the conservatism of NCSs, stochastic process such as Markovian jump is introduced in [23]. To avoid the collapse caused by NCSs attacks such as denial-of-service (DoS), deception and replay, contributions of [24]–[26] are delivered, which offer feasible solutions to these issues. It should be mentioned that

The associate editor coordinating the review of this article and approving it for publication was Bing Li.

ETS may lead to a loss of information of the systems, which motivates our study.

Inevitable faults such as sensor bias and drift happen widely, which can lead to a breakdown of the systems. To maintain the normal operation, and ensure the good performance of the NCSs, fault detection (FD) is of significance in various practical fields. The observer or filter based residual generator performs very well in terms of detection performance with the utilization of the fault alarming apparatus in [27], which is generated by making the comparison between the threshold and residual. Fault detection and isolation (FDI) established in ETS is more complex because of dynamics changes brought by the non-periodic sampling [28]. Except for discrete-time linear time invariant (LTI) systems [29], FD with ETS also performs well in complex systems such as nonlinear polynomial fuzzy NCSs [30], and aircraft systems [31]. In [32], the subspace identification method (SIM) and ETS are combined in process monitoring and the hot strip mill process (HSMP). However, unknown inputs such as disturbances should not be ignored since it would lead to a poor detection performance.

To overcome this problem, a tradeoff approach, which providing an optimal strategy is adopted, and the ratio-type performance index is utilized in many systems. In terms of the fuzzy systems with disturbance, the design of fault detection observer is converted to an  $H_-/H_\infty$  problem in [33]. For LTI systems with uniformed quantization and non-uniform quantization of output, the quantization error is regarded as the unknown input of the generated residual in [34]. The tradeoff approach is extended in event-triggered systems [35], where the event-triggered transmission errors are taken into account. Nevertheless, little literature mentioned avoiding decline of the detection accuracy because of the information missing partly introduced by ETS, and that sparks our research.

ETS is always shown as a single condition, and the trigger instants are only related to the last transmitted values. Paper [15] develops a new ETS, which replaces a single trigger condition with a set of trigger conditions, and the values in these conditions are based on the state of the past time within the specified horizon instead of the last triggered instants. Nevertheless, as far as we know, there is no existing literature which addresses the ETS based optimal FD with a set of trigger conditions.

Motivated by the above discussion, in this work, we address the tradeoff approach of optimal FD with ETS, triggers are determined by a set of conditions instead of a single condition, and the values in these conditions are not only the last transmitted data, but also the data in the past period of time. A time-varying threshold will be delivered by FDI, which can detect faults as accurately as possible, and show robustness to disturbances simultaneously, where transmission errors are taken into account. Finally, numerical simulation and application in closed-loop continuous stirred-tank reactor(CSTR) are utilized to prove the approach.

The rest of the paper is revealed below. Description and problem preliminaries of the systems are presented in Section II. The solution of optimization problem and residual generation are addressed in Section III. In Section IV, two simulation examples are given to prove the superiority of the proposed method. The conclusion is presented in Section V.

**Notations:**  $\mathbb{R}^n$  refers the  $n$ -dimensional Euclidean space;  $\|x\|_2 = \sqrt{\sum_{k=0}^{\infty} x^T(k)x(k)}$  is the  $\mathcal{L}_2$  norm, the set of signals with a finite  $\mathcal{L}_2$  norm of  $x$  is represented as  $\mathcal{L}_2^s$ ;  $\|x(k)\|_{RMS} = \sqrt{\frac{1}{N} \sum_{i=0}^{N-1} x^T(i)x(i)}$  represents the root mean square (RMS) value, where  $N$  is the number of the sliding time window;  $\mathbb{RH}_\infty$  is a real domain containing all stable transfer matrices;  $\|G(z)\|_\infty$  refers the  $\mathbb{H}_\infty$  norm of transfer matrix  $G(z)$ ;  $G^*(e^{j\theta})$  is the conjugate of  $G(e^{j\theta})$ .

## II. SYSTEMS DESCRIPTION AND PROBLEM PRELIMINARIES

### A. SYSTEMS DESCRIPTION

The discrete closed-loop system is considered as

$$\begin{cases} x(k+1) = Ax(k) + Bu(k) + B_1\omega(k) + B_2f(k) \\ y(k) = Cx(k) + Du(k) + D_1\omega(k) + D_2f(k) \end{cases} \quad (1)$$

where  $x(k) \in \mathbb{R}^n$  is the system state,  $u(k)$  is the control input,  $\omega(k)$  is the unknown disturbance,  $f(k)$  is the fault vector to be detected,  $y(k) \in \mathbb{R}^m$  is the actual output,  $A, B, B_1, B_2, C, D, D_1$  and  $D_2$  are constant matrices with compatible dimensions.

In consideration of the FDI system in this paper, an assumption needs to be presented.

*Assumption 1:*  $(A, C)$  is detectable, where  $A$  is Schur stable.

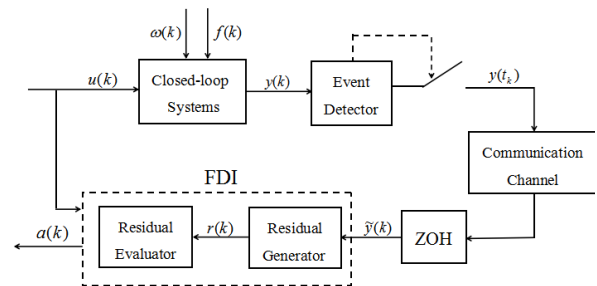


FIGURE 1. Structure of NCSs with FDI and ETS.

To realize the FD of the systems, as presented in Fig. 1, the ETS is introduced into the design of the residual generator. The major difference between our work and others is that the ETS are implemented in two steps. The first step of the ETS is given as follows:

$$\|y(t_k) - y(t_k + i)\| \leq \sigma_1 \|y(t_k + i)\| \quad (2)$$

where  $\sigma_1 \geq 0$  is the triggering parameter,  $k$  is the sampling instant,  $y(t_k)$  is the last transmitted output at instant  $t_k$ , and  $i = 1, 2, \dots, (t_{k+1} - t_k)$ . If (2) is violated, the current output  $y(t_{k+1})$  will be converted to a uniform signal  $\tilde{y}(k)$  via ZOH

and transmitted to the FD structure such that

$$\|\tilde{y}(k) - y(k)\| \leq \sigma_1 \|y(k)\| \quad (3)$$

If (2) is not violated, then check the norm of the outputs from the instant  $(k - n + 1)$  to the instant  $k$ . If the data keeps increasing or decreasing within the range, and the first inequality in (4) is violated, then we judge that a fault occurs, and the output at instant  $k$  will be delivered. The conditions of the second step are expressed as follows

$$\frac{\|y(k) - y(k - n + 1)\|}{n} \leq \sigma_2 \|y(k - n + 1)\| \quad (4)$$

where

$$\|y(k)\| \leq \|y(k - 1)\| \leq \dots \leq \|y(k - n + 1)\|$$

or

$$\|y(k)\| \geq \|y(k - 1)\| \geq \dots \geq \|y(k - n + 1)\|$$

then, the current output is converted to a uniform signal  $\tilde{y}(k)$  such that

$$\frac{\|\tilde{y}(k) - y(k)\|}{n} \leq \sigma_2 \|y(k)\| \quad (5)$$

variable  $\alpha(k)$  is utilized to denote the condition which is triggered, and is shown as follows

$$\alpha(k) = \begin{cases} 1, & \text{if (2) is triggered} \\ 0, & \text{if (4) is triggered} \end{cases} \quad (6)$$

The transmitted output is delivered to the residual generator to get the residual value  $r(k)$ , which is produced by utilizing the measurement and estimation value. The residual generator is designed as follows

$$\begin{cases} \hat{x}(k + 1) = A\hat{x}(k) + Bu(k) + L(\tilde{y}(k) - \hat{y}(k)) \\ \hat{y}(k) = C\hat{x}(k) + Du(k) \\ r(k) = T(k)(\tilde{y}(k) - \hat{y}(k)) \end{cases} \quad (7)$$

where  $\hat{x}(k) \in \mathbb{R}^n$  is the estimation state,  $\hat{y}(k) \in \mathbb{R}^m$  is the estimation output,  $L \in \mathbb{R}^{n \times m}$  is the observer gain matrix,  $T(k)$  is the impulse response matrix, both  $L$  and  $T(k)$  are undetermined coefficient matrices.

To distinguish faults from unknown inputs, the generated residual needs to be processed and compared with the threshold to decide whether a fault generates. Then, a time-varying threshold is determined as follows

$$\begin{aligned} \mathcal{J}(k) &\triangleq \|r(k)\|_{RMS} \\ \mathcal{J}_{th} &\triangleq \sup_{\omega \neq 0, u \neq 0, f = 0} \mathcal{J}(k) \end{aligned} \quad (8)$$

According to [35], the criteria is specified as follows

$$\begin{cases} \mathcal{J}(k) \leq \mathcal{J}_{th} \Rightarrow a(k) = 0, & \text{normal} \\ \mathcal{J}(k) > \mathcal{J}_{th} \Rightarrow a(k) = 1, & \text{a fault generates} \end{cases}$$

where  $\|r(k)\|_{RMS}$  stands for the evaluation function,  $\mathcal{J}_{th}$  is the time-varying threshold which needs to be determined, and  $a(k)$  indicates the alert status. The estimation error is defined

as  $e(k) = x(k) - \hat{x}(k)$ , and the transmission error of ETS is defined as  $\tilde{e}(k) = \tilde{y}(k) - y(k)$ . Combining (1) and (6), an error model is established as follows

$$\begin{cases} e(k + 1) = (A - LC)e(k) + (B_1 - LD_1)\omega(k) \\ \quad + (B_2 - LD_2)f(k) - L\tilde{e}(k) \\ r(k) = T(k)[Ce(k) + D_1\omega(k) + D_2f(k) + \tilde{e}(k)] \end{cases} \quad (9)$$

Then, take  $\mathcal{Z}$  transformation of (9), define

$$\begin{aligned} G_\omega(z) &= D_1 + C(zI - (A - LC))^{-1}(B_1 - LD_1) \\ G_f(z) &= D_2 + C(zI - (A - LC))^{-1}(B_2 - LD_2) \\ G_{\tilde{e}}(z) &= I - C(zI - (A - LC))^{-1}L \end{aligned}$$

then  $r(k)$  can be formulated as

$$r(z) = T(z)[G_\omega(z)\omega(z) + G_f(z)f(z) + G_{\tilde{e}}(z)\tilde{e}(z)] \quad (10)$$

## B. PROBLEM PRELIMINARIES

In an attempt to measure the robustness of the residual generator against disturbances and the sensitivity to faults, the optimization indices which provide a compromise can be utilized. To assess robustness of the FDI against disturbances, let  $f = 0$  and  $u = 0$ , by utilizing (3) and (5), the following inequality is acquired

$$\begin{aligned} \|r_\omega(k)\|_2 &= \sup_{f=0, u=0} \|r(k)\|_2 \\ &\leq \|TG_\omega\|_\infty \|\omega(k)\|_2 + \|TG_{\tilde{e}}\|_\infty \|\tilde{e}(k)\|_2 \\ &\leq \|TG_\omega\|_\infty \|\omega(k)\|_2 + \sigma \|TG_{\tilde{e}}\|_\infty \|y(k)\|_2 \\ &\leq \|TG_\omega\|_\infty \|\omega(k)\|_2 + \sigma \varphi_1 \|TG_{\tilde{e}}\|_\infty \|\omega(k)\|_2 \\ &\leq 2\|T[G_\omega \ \sigma \varphi_1 \ G_{\tilde{e}}]\|_\infty \|\omega(k)\|_2 \end{aligned}$$

where  $\varphi_1 = \|G_1\|_\infty$ ,  $G_1(z) = D_1 + C(zI - A)^{-1}B_1$ , and  $\sigma = \alpha(k)\sigma_1 + (1 - \alpha(k))n\sigma_2$ .

Similarly, let  $\omega(k) = 0$ , and  $u(k) = 0$ , then, the sensitivity to faults is evaluated by utilizing the (3) and (5), such that

$$\begin{aligned} \|r_f(k)\|_2 &= \sup_{\omega=0, u=0} \|r(k)\|_2 \\ &\leq 2\|T[G_f \ \sigma \varphi_2 \ G_{\tilde{e}}]\|_\infty \|f(k)\|_2 \end{aligned}$$

where  $\varphi_2 = \|G_2\|_\infty$ ,  $G_2(z) = D_2 + C(zI - A)^{-1}B_2$ ,  $\sigma = \alpha(k)\sigma_1 + (1 - \alpha(k))n\sigma_2$ .

According to [35], a ratio-type performance index is employed for the residual generator (10) such that

$$\min_{L, T(z)} \mathcal{J}_{rs}(L, T(z)) = \min_{L, T(z)} \frac{\|T(z)[G_\omega \ \sigma \varphi_1 \ G_{\tilde{e}}(z)]\|_\infty}{\|T(z)[G_f \ \sigma \varphi_2 \ G_{\tilde{e}}(z)]\|_\infty} \quad (11)$$

For simplicity without loss of universality,  $T(z)$  is specified as a constant matrix  $W$ . Then, the ratio-type performance index turns into as follows

$$\min_{L, W} \mathcal{J}_{rs}(L, W) = \min_{L, W} \frac{\|W[G_\omega \ \sigma \varphi_1 \ G_{\tilde{e}}(z)]\|_\infty}{\|W[G_f \ \sigma \varphi_2 \ G_{\tilde{e}}(z)]\|_\infty} \quad (12)$$

Then, our targets are transformed into the following works

- 1) Acquiring the optimal observer gain  $L_{min}$  and the weighting matrix  $W_{min}$  for the optimization problem in (12).
- 2) Specifying the threshold  $\mathcal{J}_{th}$  by assessing the effects of  $\omega(k)$  and  $\tilde{e}(k)$  on the function  $\|r(k)\|_{RMS}$  in the case of  $f(k) = 0$ .

### III. MAIN RESULTS

#### A. OPTIMAL RESIDUAL GENERATOR DESIGN

The optimal solution of (12) and residual generator of the FD will be presented in this section. To proceed successfully, a lemma needs to be introduced in advance.

*Lemma 1:* [36] Suppose that the discrete-time LTI systems  $G(z) = D + C(zI - A)^{-1}B \in \mathbb{RH}_\infty$  has no transmission zeros on the unit circle. Then, there exists a co-inner-outer factorization of  $G(z) = G_{co}(z)G_{ci}(z)$ , with the co-inner  $G_{ci}(z)$  satisfying  $G_{ci}(e^{j\theta})G_{ci}^*(e^{j\theta}) = I$  and

$$\begin{aligned} G_{co}(z) &= H + C(zI - A)^{-1}LH, \\ G_{ci}(z) &= H^\dagger D + H^\dagger C(zI - (A - LC))^{-1}(B - LD), \\ L &= (AXC^T + BD^T)(CXC + DD^T)^{-1} \end{aligned}$$

where  $X$  is the stabilization solution of the discrete-time Riccati equation (DTRE)

$$\begin{aligned} AXA^T - X + BB^T - (AXC^T + BD^T) \\ (CXC^T + DD^T)^{-1}(CXA^T + DB^T) = 0 \end{aligned}$$

and  $H^\dagger$  is left inverse of the  $H$  satisfying  $H^\dagger H = I$  and  $HH^T = CXC^T + DD^T$ . What's more, the  $\mathbb{RH}_\infty$  left inverse of  $G_{co}(z)$  is given by

$$G_{co}^\dagger = H^\dagger - H^\dagger C(zI - (A - LC))^{-1}L$$

*Theorem 1:* For the given LTI systems (1) with ETS (2) and (4) and the residual generator (7),

$$\begin{aligned} L_{min} &= (AXC^T + B_1 D_1^T)(CXC^T + D_1 D_1^T + \sigma^2 \varphi_1^2 I)^{-1} \\ W_{min} &= H^\dagger \end{aligned} \quad (13)$$

is the optimization solution for problem (12), where  $X$  is the stabilization solution of the following DTRE

$$\begin{aligned} AXA^T - X + B_1 B_1^T - (AXC^T + B_1 D_1^T) \\ (CXC^T + D_1 D_1^T + \sigma^2 \varphi_1^2 I)^{-1}(CXA^T + D_1 B_1^T) = 0 \end{aligned} \quad (14)$$

where  $\sigma = \alpha(k)\sigma_1 + (1 - \alpha(k))n\sigma_2$ , and  $H$  satisfies  $HH^T = CXC^T + D_1 D_1^T + \sigma^2 \varphi_1^2 I$ .

*proof 1:* Define the system

$$\begin{aligned} G_{\omega\tilde{e},L}(z) &= [G_\omega(z) \ \sigma\varphi_1 G_{\tilde{e}}(z)] \\ &= [D_1 \ \sigma\varphi_1 I] + C(zI - (A - LC))^{-1} \\ &\quad [B_1 - LD_1 \ \ -\sigma\varphi_1 L]. \end{aligned}$$

In a similar way,  $G_{f\tilde{e},L} = [D_2 \ \sigma\varphi_2 I] + C(zI - (A - LC))^{-1}[B_2 - LD_2 \ \ \sigma\varphi_2 L]$  is obtained. Then the co-inner-outer factorization technique is utilized and  $G_{d\tilde{e},L}(z) = G_{\omega co}(z)G_{\omega ci}(z)$  is obtained, where  $G_{\omega co}(z)$  is the co-outer factor and  $G_{\omega ci}(z)$  is the co-inner factor satisfying  $G_{\omega ci}(e^{j\theta})G_{\omega ci}^*(e^{j\theta}) = I$ . Let  $T(z) = M(z)G_{\omega co}^\dagger(z)$  with an arbitrary systems  $M(z) \in \mathbb{RH}_\infty$ . Then, optimal solution of  $T(z)$  can be expressed as

$$\begin{aligned} \mathcal{J}_{rs}(T(z)) &= \frac{\|T(z)G_{\omega\tilde{e},L}(z)\|_\infty}{\|T(z)G_{f\tilde{e},L}(z)\|_\infty} \\ &= \frac{\|M(z)\|_\infty}{\|M(z)G_{\omega co}^\dagger G_{f\tilde{e},L}(z)\|_\infty} \end{aligned}$$

$$\geq \frac{1}{\|G_{\omega co}^\dagger(z)G_{f\tilde{e},L}(z)\|_\infty}$$

Specifying  $M(z)$  as an identity matrix, then,  $T(z) = G_{\omega co}^\dagger$  is the optimal solution of problem (12), according to the Lemma 1, the  $G_{\omega co}^\dagger(z)$  is shown as follows

$$\begin{aligned} G_{\omega co}^\dagger(z) &= H^\dagger - H^\dagger C[zI - ((A - LC) - L_0 C)]^{-1}L_0 \\ L_0 &= [(A - LC)XC^T + (B_1 - LD_1)D_1^T - \sigma^2 \varphi_1^2 L] \\ &\quad (CXC^T + D_1 D_1^T + \sigma^2 \varphi_1^2 I)^{-1} \end{aligned}$$

where  $X$  is the stabilization solution of the DTRE

$$\begin{aligned} (A - LC)X(A - LC)^T - X + (B_1 - LD_1)(B_1 - LD_1)^T \\ + \sigma^2 \varphi_1^2 LL^T - \Lambda(CXC^T + D_1 D_1^T + \sigma^2 \varphi_1^2 I)^{-1}\Lambda^T = 0 \end{aligned} \quad (15)$$

and

$$\begin{aligned} \sigma &= \alpha(k)\sigma_1 + (1 - \alpha(k))n\sigma_2 \\ \Lambda &= (A - LC)XC^T + (B_1 - LD_1)D_1^T - \sigma^2 \varphi_1^2 L \end{aligned}$$

The (15) can be expanded, then, the DTRE in (15) is equivalent to the one in (14). Let  $L_0 = L_{min} - L$ . If  $L_0 = 0$ ,  $L_{min} = L$ , and  $G_{\omega co}^\dagger$  becomes the constant weighting matrix  $H^\dagger$ , then  $W_{min} = H^\dagger$  is specified as the optimal solution of (11). By replacing  $L$  with  $L_{min}$ , the following expressions

$$\min_{T(z)} \frac{\|T(z)G_{\omega\tilde{e},L_{min}(z)}\|_\infty}{\|T(z)G_{f\tilde{e},L_{min}(z)}\|_\infty} = \frac{\|W_{min}G_{\omega\tilde{e},L_{min}(z)}\|_\infty}{\|W_{min}G_{f\tilde{e},L_{min}(z)}\|_\infty} \quad (16)$$

and

$$\begin{aligned} G_{\omega\tilde{e},L}(z) &= K^{-1}G_{\omega\tilde{e},L_{min}}(z) \\ G_{f\tilde{e},L}(z) &= K^{-1}G_{f\tilde{e},L_{min}}(z) \end{aligned} \quad (17)$$

are obtained with the application of left co-prime factorization technique, where  $K(z) = I - C(zI - (A - L_{min}C))^{-1}(L_{min} - L)$  is left invertible. Then, the following inequality is acquired according to the left side of (16) such that

$$\begin{aligned} \min_{T(z)} \frac{\|T(z)G_{\omega\tilde{e},L_{min}(z)}\|_\infty}{\|T(z)G_{f\tilde{e},L_{min}(z)}\|_\infty} &= \min_{T(z)} \frac{\|T(z)K(z)G_{\omega\tilde{e},L}(z)\|_\infty}{\|T(z)K(z)G_{f\tilde{e},L}(z)\|_\infty} \\ \min_{\hat{T}(z)} \frac{\|\hat{T}(z)G_{\omega\tilde{e},L}(z)\|_\infty}{\|\hat{T}(z)G_{f\tilde{e},L}(z)\|_\infty} &\leq \min_W \frac{\|WG_{\omega\tilde{e},L}(z)\|_\infty}{\|WG_{f\tilde{e},L}(z)\|_\infty} \end{aligned} \quad (18)$$

and

$$\frac{\|W_{min}G_{\omega\tilde{e},L_{min}(z)}\|_\infty}{\|W_{min}G_{f\tilde{e},L_{min}(z)}\|_\infty} \leq \min_{L,W} \frac{\|WG_{\omega\tilde{e},L}(z)\|_\infty}{\|WG_{f\tilde{e},L}(z)\|_\infty} \quad (19)$$

which means that (13) is the optimal solution of (12).

Then, the minimum value of the performance index  $\mathcal{J}_{rs}(L, W)$  is expressed as

$$\mathcal{J}_{rs \ min} = \frac{1}{\|H^\dagger G_{f\tilde{e},L_{min}}(z)\|_\infty} \quad (20)$$

**B. THRESHOLD GENERATION AND RESIDUAL EVALUATION**

Residual evaluation plays a significant role in distinguishing the faults from the unknown inputs such as disturbances and transmission errors. The norm-based RMS value selected as the evaluation function is widely accepted [33]. In this work, the threshold is defined as the maximum impact of disturbances and transmission errors, which are actually affected by the input  $u(k)$  on the evaluation function under the assumption of  $f(k) = 0$ . Therefore, the threshold is indicated as

$$\begin{aligned} \|r_{\omega\tilde{e}}(k)\|_{RMS} &= \|r_{\omega}(k) + r_u(k)\|_{RMS} \\ &\leq \|r_{\omega}(k)\|_{RMS} + \|r_u(k)\|_{RMS} \end{aligned} \quad (21)$$

where  $r_{\omega\tilde{e}}(k) = r(k)|_{f=0}$ ,  $r_{\omega}(k) = r(k)|_{f=0, u=0}$ , and  $r_u(k) = r(k)|_{f=0, \omega=0}$ , the threshold  $J_{th}$  is specified as

$$J_{th} = J_{th,\omega} + J_{th,u} \quad (22)$$

where

$$\begin{aligned} J_{th,\omega} &= \sup_{\omega} \|r_{\omega}(k)\|_{RMS}, \\ J_{th,u} &= \sup_u \|r_u(k)\|_{RMS}. \end{aligned}$$

The threshold  $J_{th}$  is time-varying and could be computed online according to (22). Define an augmenting vector  $\tilde{x}(k) = [x^T(k) \hat{x}^T(k) e^T(k)]^T$ . Then, the system (1), residual generator (7), error system (9), and the optimal solution (13) are integrated into the following augmenting system

$$\begin{cases} \tilde{x}(k+1) = \bar{A}x(k) + \bar{B}u(k) + \bar{B}_1\omega(k) + \bar{L}\tilde{e}(k) \\ r(k) = \bar{C}x(k) + W_{min}D_1\omega(k) + W_{min}\tilde{e}(k) \end{cases} \quad (23)$$

where

$$\begin{aligned} \bar{A} &= \begin{bmatrix} A & 0 & 0 \\ 0 & A & L_{min}C \\ 0 & 0 & A - L_{min}C \end{bmatrix}, \quad \bar{B} = \begin{bmatrix} B \\ B \\ 0 \end{bmatrix} \\ \bar{B}_1 &= \begin{bmatrix} B_1 \\ L_{min}D_1 \\ B_1 - L_{min}D_1 \end{bmatrix}, \quad \bar{L} = \begin{bmatrix} 0 \\ L_{min} \\ -L_{min} \end{bmatrix} \\ \bar{C} &= [0 \quad 0 \quad W_{min}C] \end{aligned}$$

The theorem of the threshold is given as follows.

**Theorem 2:** For given matrices  $\bar{A}$ ,  $\bar{B}$ ,  $\bar{B}_1$ ,  $\bar{L}$  and  $\bar{C}$ , and the residual generator (7) with the optimal solution (13), if there exist nonnegative scalars  $\gamma_1$ ,  $\gamma_2$ ,  $\mu_1$ , and  $\mu_2$  and positive definite matrices  $P_1$  and  $P_2$  of appropriate dimensions satisfying the following inequalities

$$\begin{bmatrix} \Gamma_{11} & \Gamma_{12} & \Gamma_{13} \\ * & \Gamma_{22} & \Gamma_{23} \\ * & * & \Gamma_{33} \end{bmatrix} \leq 0 \quad (24)$$

$$\begin{bmatrix} \Theta_{11} & \Theta_{12} & \Theta_{13} \\ * & \Theta_{22} & \Theta_{23} \\ * & * & \Theta_{33} \end{bmatrix} \leq 0 \quad (25)$$

where

$$\Gamma_{11} = \bar{A}^T P_1 \bar{A} + \bar{A}^T Q_1 \bar{A} - P_1 - Q_1 + \bar{C}^T \bar{C} + \mu_1 \sigma^2 \bar{C}^T \bar{C}$$

$$\begin{aligned} \Gamma_{12} &= \bar{A}^T P_1 \bar{B}_1 + \bar{A}^T Q_1 \bar{B}_1 + \bar{C}^T W_{min} D_1 + \mu_1 \sigma^2 \bar{C}^T D_1 \\ \Gamma_{13} &= \bar{A}^T P_1 \bar{L} + \bar{A}^T Q_1 \bar{L} + \bar{C}^T W_{min} \\ \Gamma_{22} &= \bar{B}_1^T P_1 \bar{B}_1 + \bar{B}_1^T Q_1 \bar{B}_1 + (W_{min} D_1)^T (W_{min} D_1) \\ &\quad + \mu_1 \sigma^2 D_1^T D_1 - \gamma_1^2 I \\ \Gamma_{23} &= \bar{B}_1^T P_1 \bar{L} + \bar{B}_1^T Q_1 \bar{L} + (W_{min} D_1)^T W_{min} \\ \Gamma_{33} &= \bar{L}^T P_1 \bar{L} + \bar{L}^T Q_1 \bar{L} + W_{min}^T W_{min} - \mu_1 I \\ \Theta_{11} &= \bar{A}^T P_2 \bar{A} + \bar{A}^T Q_2 \bar{A} - P_2 - Q_2 + \bar{C}^T \bar{C} + \mu_2 \sigma^2 \bar{C}^T \bar{C} \\ \Theta_{12} &= \bar{A}^T P_2 \bar{B} + \bar{A}^T Q_2 \bar{B} + \mu_2 \sigma^2 \bar{C}^T D \\ \Theta_{13} &= \bar{A}^T P_2 \bar{L} + \bar{A}^T Q_2 \bar{L} + \bar{C}^T W_{min} \\ \Theta_{22} &= \bar{B}^T P_2 \bar{B} + \bar{B}^T Q_2 \bar{B} + \mu_2 \sigma^2 D^T D - \gamma_2^2 I \\ \Theta_{23} &= \bar{B}^T P_2 \bar{L} + \bar{B}^T Q_2 \bar{L} \\ \Theta_{33} &= \bar{L}^T P_2 \bar{L} + \bar{L}^T Q_2 \bar{L} + W_{min}^T W_{min} - \mu_2 I \\ \bar{C} &= [C \quad 0 \quad 0] \\ \sigma &= \alpha(k)\sigma_1 + (1 - \alpha(k))n\sigma_2 \end{aligned}$$

then the augmenting system in (23) satisfying the  $\mathbb{H}_{\infty}$  performance index  $\|r_{\omega}(k)\|_2 \leq \gamma_1 \|\omega(k)\|_2$ , and  $\|r_u(k)\|_2 \leq \gamma_2 \|u(k)\|_2$ , and the threshold is given as follows

$$J_{th} = \frac{\gamma_1 \min}{\sqrt{N}} \|\omega(k)\|_2 + \gamma_2 \min \|u(k)\|_2 \quad (26)$$

where  $\gamma_1 \min = \min(\gamma_1)$ ,  $\gamma_2 \min = \min(\gamma_2)$ .

*proof 2:* Considering the  $\mathcal{L}_2$  gain from  $\omega(k)$  to  $r(k)$ , let  $u(k) = 0$ , then according to (3) and (5), the following inequality is obtained if nonnegative scalar  $\mu_1$  exists.

$$\begin{aligned} \mu_1 \tilde{e}^T(k) \tilde{e}(k) &\leq \mu_1 \sigma_1^2 y^T(k) y(k) \\ &\leq \mu_1 \sigma_1^2 [x^T(k) C^T C x(k) + 2x^T(k) C^T D_1 \omega(k) \\ &\quad + \omega^T(k) D_1^T D_1 \omega(k)] \\ &= \mu_1 \sigma^2 [\bar{x}^T(k) \bar{C}^T \bar{C} \bar{x}(k) + 2\bar{x}^T(k) \bar{C}^T D_1 \omega(k) \\ &\quad + \omega^T(k) D_1^T D_1 \omega(k)] \end{aligned} \quad (27)$$

where

$$\sigma = \alpha(k)\sigma_1 + (1 - \alpha(k))n\sigma_2$$

Define a Lyapunov functional

$$V(k) = \bar{x}^T(k) P_1 \bar{x}(k) + \bar{x}^T(k) Q_1 \bar{x}(k)$$

and the function

$$\mathcal{J} = \Delta V(k) + r_{\omega}^2(k) r_{\omega}(k) - \gamma_1^2 \omega^T(k) \omega(k)$$

where

$$\begin{aligned} \Delta V(k) &= V(k+1) - V(k) \\ &= \bar{x}^T(k) \bar{A}^T P_1 \bar{A} \bar{x}(k) + \bar{x}^T(k) \bar{A}^T Q_1 \bar{A} \bar{x}(k) \\ &\quad + 2\bar{x}^T(k) \bar{A}^T P_1 \bar{B}_1 \omega(k) + 2\bar{x}^T(k) \bar{A}^T Q_1 \bar{B}_1 \omega(k) \\ &\quad + 2\bar{x}^T(k) \bar{A}^T P_1 \bar{L} \tilde{e}(k) + 2\bar{x}^T(k) \bar{A}^T Q_1 \bar{L} \tilde{e}(k) \\ &\quad + \omega^T(k) \bar{B}_1^T P_1 \bar{B}_1 \omega(k) + \omega^T(k) \bar{B}_1^T Q_1 \bar{B}_1 \omega(k) \\ &\quad + 2\omega^T(k) \bar{B}_1^T P_1 \bar{L} \tilde{e}(k) + 2\omega^T(k) \bar{B}_1^T Q_1 \bar{L} \tilde{e}(k) \\ &\quad + \tilde{e}^T(k) \bar{L}^T P_1 \bar{L} \tilde{e}(k) + \tilde{e}^T(k) \bar{L}^T Q_1 \bar{L} \tilde{e}(k) \\ &\quad - \bar{x}^T(k) P_1 \bar{x}(k) - \bar{x}^T(k) Q_1 \bar{x}(k) \end{aligned}$$

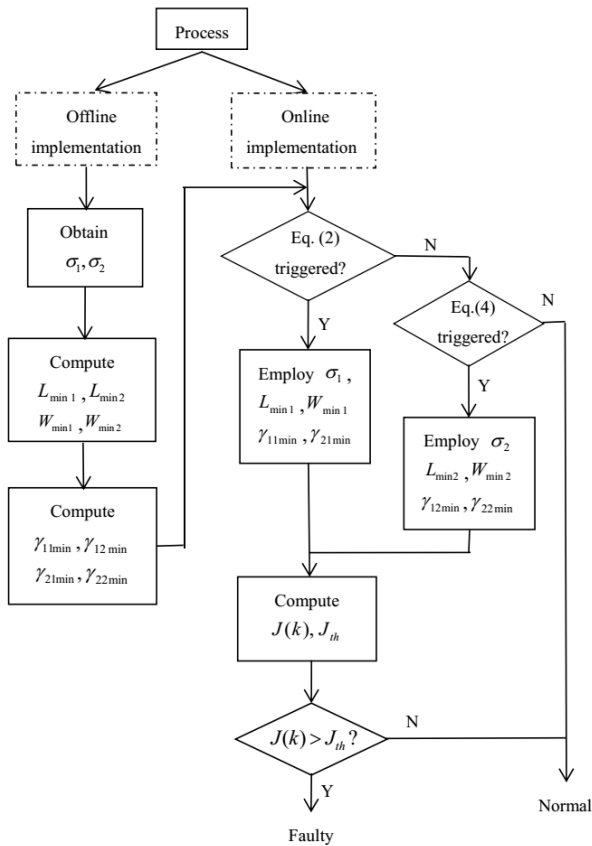


FIGURE 2. Procedure for optimal FD with ETS.

Adding the (27) into  $\mathcal{J}$ , then

$$\begin{aligned} \mathcal{J} \leq & 7\Delta V(k) - \gamma_1^2 \omega^T(k)\omega(k) + \bar{x}^T(k)\bar{C}^T\bar{C}(k) \\ & + 2\bar{x}^T(k)\bar{C}^T W_{min}D_1(k) + 2\bar{x}^T(k)\bar{C}^T W_{min}\tilde{e}(k) \\ & + \omega^T(k)(W_{min}D_1)^T(W_{min}D_1)\omega(k) \\ & + 2\omega^T(W_{min}D_1)^T W_{min}\tilde{e}(k) + \tilde{e}^T(k)W_{min}^T W_{min}\tilde{e}(k) \\ & - \mu_1 \tilde{e}^T(k)\tilde{e}(k) + \mu_1 \sigma^2 [\bar{x}^T(k)\bar{C}^T\bar{C}\bar{x}(k) \\ & + 2\bar{x}^T(k)\bar{C}^T D_1\omega(k) + \omega^T(k)D_1^T D_1\omega(k)] \end{aligned} \quad (28)$$

define a vector

$$\zeta(k) = [\bar{x}^T(k) \quad \omega^T(k) \quad \tilde{e}^T(k)]^T$$

then (28) can be described as  $\mathcal{J} \leq \zeta^T(k)\Gamma\zeta(k)$ .

If (24) holds,  $\mathcal{J} \leq 0$ , then, for any zero initial states,  $\sum_{k=0}^{\infty} \mathcal{J}(k) \leq 0$  proves that the  $\mathbb{H}_{\infty}$  performance index of  $\|r_u(k)\|_2 \leq \gamma_1 \|\omega(k)\|_2$  is obtained.

Similarly, considering  $\omega(k) = 0$ . Defining a Lyapunov functional  $V(k) = \bar{x}^T(k)P_2\bar{x}(k) + \bar{x}^T(k)Q_2\bar{x}(k)$ , then the  $\mathbb{H}_{\infty}$  index of  $\|r_u(k)\|_2 \leq \gamma_2 \|u(k)\|_2$  is obtained if (25) holds.

Known from [35],  $\omega(k) \in \mathcal{L}_2^2$ , then  $\|\omega(k)\| \leq \frac{\|\omega(k)\|_2}{\sqrt{N}}$ . For  $\|u(k)\|_2 \leq \infty$ , by the definition of the RMS, the  $\mathcal{L}_2$  gain equals to the RMS gain, then  $\|r_u(k)\|_2 \leq \gamma_2 \|u(k)\|_2$ , then (26) is obtained. The whole procedure in this paper is proposed in Fig. 2.

#### IV. SIMULATION

In this section, a numerical simulation and application on CTSR will be used to verify the proposed approach.

##### A. NUMERICAL SIMULATION

Consider a LTI systems, which data is given as follows

$$\begin{aligned} A &= \begin{bmatrix} 0.1 & 1 \\ 0 & 0.3 \end{bmatrix}, & B &= \begin{bmatrix} 0.2 \\ -1 \end{bmatrix}, \\ C &= \begin{bmatrix} 1 & 0 \\ 0 & 1 \end{bmatrix}, & D &= \begin{bmatrix} 0.3 \\ 0.5 \end{bmatrix}, \\ B_1 &= \begin{bmatrix} 1 & 1 & 0 \\ 0 & 2 & -1 \end{bmatrix}, & D_1 &= \begin{bmatrix} 0.4 & 0 & 0 \\ 0 & -1 & 0.6 \end{bmatrix}. \end{aligned}$$

Referring to [35], let  $B_2 = B, D_2 = D, h = 0.1$  is the sampling period, and fault is defined as follows

$$f(k) = \begin{cases} \frac{\pi}{12}, & 0 \leq k \leq 100 \\ 0, & otherwise \end{cases}$$

the time-varying input  $u(k)$  is given as

$$u(k) = \frac{\pi}{15} \sin(0.2k), \quad 0 \leq k \leq 100$$

the disturbance  $\omega(k)$  is defined as the white noise.

According to (13) and (14),  $L_{min}$  and  $W_{min}$  can be obtained, the differences between our work and [35] is that the  $L_{min}$  and the  $W_{min}$  change the  $\sigma_1$  and  $\sigma_2$  instead of remaining fixed, choose  $\sigma_1 = 0.2, \sigma_2 = 0.02$ , and  $n = 5$ , then the following parameters can be obtained

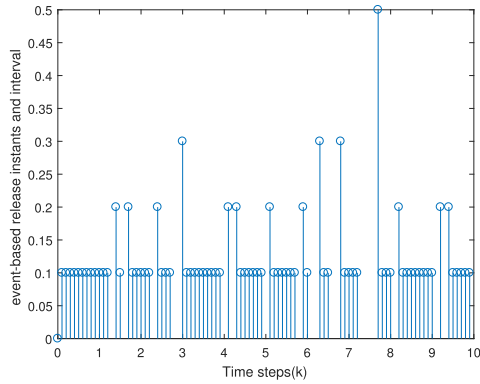
$$\begin{aligned} L_{min1} &= \begin{bmatrix} 0.0337 & 0.0673 \\ -0.1098 & -0.0556 \end{bmatrix}, \\ L_{min2} &= \begin{bmatrix} 0.2943 & 0.4937 \\ -0.0754 & -0.5587 \end{bmatrix}, \\ W_{min1} &= \begin{bmatrix} -2.7052 & 2.1599 \\ 2.1777 & 2.4005 \end{bmatrix}, \\ W_{min2} &= \begin{bmatrix} -2.8661 & 2.4697 \\ 2.3518 & 2.8185 \end{bmatrix}. \end{aligned}$$

The detection performance of missed detection rate (MDR) is computed as

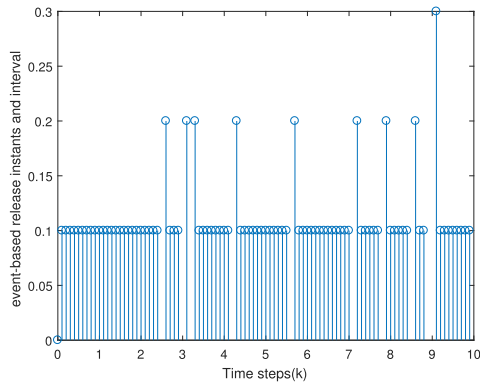
$$MDR = 1 - \frac{\text{samples}(a(k) = 1)}{\text{total samples}(faults)} \times 100\% \quad (29)$$

Select  $N = 20$  as the moving time window length, and  $\gamma_{11min} = 0.7037, \gamma_{12min} = 3.0401, \gamma_{21min} = 0.6007, \gamma_{22min} = 3.5030$ , which are computed according to (24) and (25). The event-triggered releases and the result of FD with different ETS proposed in our work are presented, and the comparison with the old one is shown in Fig. 3 and Fig. 4, where new ETS means that the ETS proposed in this work with (2) and (4), and old ETS stands for the single triggering condition of (2) with parameter  $\sigma_1$ .

Fig. 4 shows a better FD performance with new ETS than the old one. By utilizing (29), the MDR of the FD with the two kinds of ETSs are acquired. To further appreciate the



(a) old ETS



(b) new ETS

FIGURE 3. Event releases of old and new ETS.

TABLE 1. Comparison between old and new ETS.

Class	Triggers	MDR
Old ETS	77	34%
New ETS	89	13%

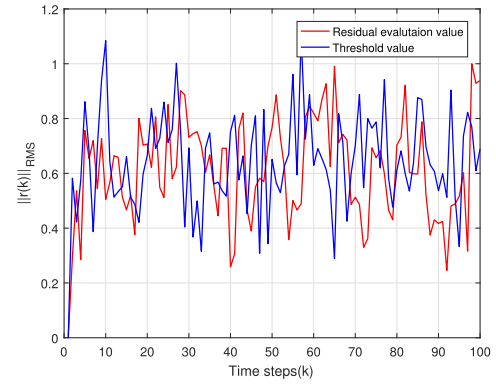
performance of new ETS, comparison between FD with two ETSs is shown in TABLE 1.

*Remark 1:* The disturbance in the model is specified as the white noise, which could reduce the conservatism. The triggers of new ETS is more than the old one since the second condition set, which means leading to an increase of the communication cost. Therefore, a tradeoff of the performance of FD and communication cost should be achieved.

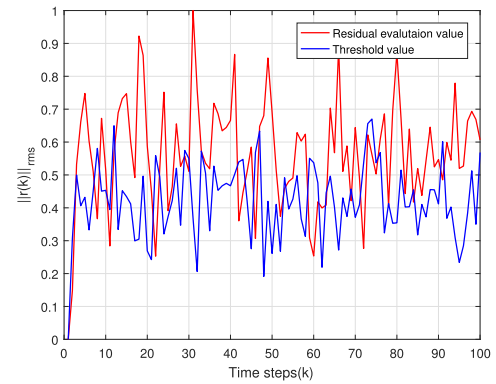
*Remark 2:* According to Theorem 2, in order to ensure the feasibility of LMI, an appropriate range of threshold  $J_{th}$  should be set by considering the actual production needs, and triggering parameter  $\sigma$  can be adjusted within the range to achieve the best tradeoff between the communication cost and FD performance.

### B. APPLICATION ON CSTR

The CSTR plays a significant role in the reaction device since it is utilized widely for various physical and chemical reactions in industrial production. Most of synthetic production reactors in the production of plastic, chemical fiber and



(a) FD with old ETS



(b) FD with new ETS

FIGURE 4. Results of FD with old and new ETS.

synthetic rubber are CSTR. In addition, it also has a wide application on the production of other industries, such as pharmaceutical, paint, and fuel.

The reaction temperature is one of the most important parameter in a CSTR since it affects product quality and yield directly. The mechanism of CSTR is complex where the characteristics such as time-varying, nonlinear, and time delay are presented, since the concentration of reactants (or catalyst), reactor pressure, heating (or cooling) device type, heat agent (or refrigerant) temperature and flow rate have a greater impact on temperature control.

Before starting reaction in CSTR, the materials and catalysts are fed to the kettle through the feed port, the reaction temperature is provided by the high-pressure steam which introduced into the reactor jacket, and the reaction temperature needs to be maintained when it reaches the set value, sometimes the further heating is required. During the stirring process, materials will be mixed uniformly and release heat, the releasing rate is related to the reaction temperature, which is measured online by the temperature sensor installed in the kettle. In addition, the shape and size of the agitator can also have an effect on the reaction. The working principle of CSTR proposed in [37] is presented in Fig. 5.

The state variables of CSTR systems are  $x = [C \ T \ T_c]^T$ , and  $x(0) = [0.1 \ 430.9 \ 416.7]^T$ , the input variables are  $u = [C_i \ T_i \ T_{ci}]^T$ , and initial input is  $u(0) = [1 \ 350 \ 350]^T$  and the

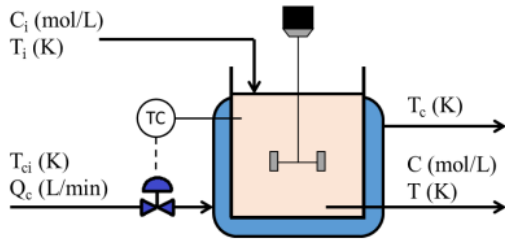


FIGURE 5. Structure of CSTR.

outputs are  $y = [C \ T \ T_c \ Q_c]^T$ , white noise is specified as disturbance, and faults are characterized by ramp signal and introduced after 200s of normal operation, parameters of the CSTR are also proposed in [37], a discrete model is obtained as form of (1) with the sampling period of 1s, and matrices with appropriate dimensions are given as follows

$$\begin{aligned}
 A &= \begin{bmatrix} 0.9942 & -0.0270 & 0.5022 \\ -0.5007 & 0.0162 & -0.0050 \\ 0.0004 & -0.0261 & -0.0077 \end{bmatrix}, \\
 B &= \begin{bmatrix} 0.0346 & 4.3515 & 4.6858 \\ -0.0062 & -2.2070 & -2.2552 \\ 0.0093 & 3.1630 & 3.2255 \end{bmatrix}, \\
 C &= \begin{bmatrix} 0.0171 & -1.0022 & 0.0030 \\ 0.0034 & 0.9032 & -0.1071 \\ -0.0019 & -0.0817 & 1.0632 \\ 0.0023 & 0.0010 & 0.0003 \end{bmatrix}, \\
 D &= \begin{bmatrix} -0.0336 & 5.0910 & 4.5602 \\ -0.0054 & -1.7987 & -1.7866 \\ 0.0047 & 1.5795 & 1.5578 \\ 0.0021 & 0.8228 & 0.8090 \end{bmatrix}, \\
 B_1 &= \begin{bmatrix} 10.2220 & 10.2220 & 10.2220 \\ 0.0708 & 0.0708 & 0.0708 \\ -0.0232 & -0.0232 & -0.0232 \end{bmatrix}, \\
 D_1 &= \begin{bmatrix} -9.6243 & -9.6243 & -9.6243 \\ -0.0308 & -0.0308 & -0.0308 \\ -0.0169 & -0.0169 & -0.0169 \\ -0.0055 & -0.0055 & 0.0055 \end{bmatrix}, \\
 B_2 &= \begin{bmatrix} -0.0001 & -0.0067 & -0.0067 \\ 0.0005 & 0.0231 & 0.0231 \\ -0.0003 & -0.0167 & -0.0167 \end{bmatrix}, \\
 D_2 &= \begin{bmatrix} -0.0310 & -1.5476 & -1.5476 \\ -0.0001 & -0.0040 & -0.0040 \\ 0.0001 & 0.0066 & 0.0066 \\ -0.0000 & -0.0008 & -0.0008 \end{bmatrix},
 \end{aligned}$$

Choosing  $n = 20$ ,  $N = 30$ , the triggering parameters are selected as  $\sigma_1 = 0.5$ ,  $\sigma_2 = 0.02$ . The optimal observer gains and weighting matrices are given as follows

$$L_{min1} = \begin{bmatrix} -0.8425 & -1.0027 & -0.0015 & -1.0005 \\ -0.0058 & -0.0103 & -0.0018 & -0.0037 \\ 0.0019 & 0.0041 & 0.0051 & 0.0029 \end{bmatrix},$$

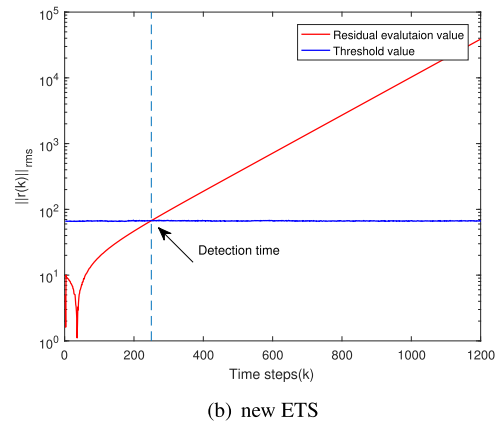
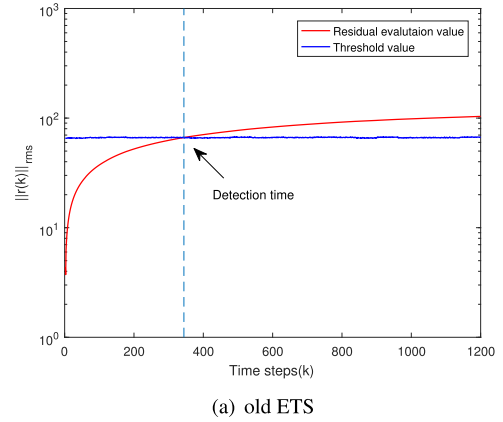


FIGURE 6. Results of FD with old and new ETS of CSTR.

$$\begin{aligned}
 L_{min2} &= \begin{bmatrix} -1.0271 & -0.8595 & 0.3622 & -0.1238 \\ -0.1967 & -0.2793 & 0.4316 & -0.0204 \\ 0.0671 & -0.5668 & 0.2348 & 0.0038 \end{bmatrix}, \\
 W_{min1} &= \begin{bmatrix} 2.0005 & 1.1197 & 1.0001 & -1.1193 \\ -1.1690 & 0.0007 & 0.0012 & -0.0001 \\ -0.0004 & -0.1193 & 0.0002 & -0.1197 \\ 0.0033 & 0.0043 & 0.1690 & 0.0021 \end{bmatrix}, \\
 W_{min2} &= \begin{bmatrix} -1.0135 & 0.1197 & 0.1330 & 0.4067 \\ -0.0135 & -0.2338 & -0.2840 & 0.1360 \\ -0.1027 & -0.2330 & 0.2691 & -0.0011 \\ 0.0741 & -0.0014 & 0.0017 & 0.0084 \end{bmatrix},
 \end{aligned}$$

By utilizing the algorithm in Fig. 2, FD performance with different ETSs and a comparison between them are proposed in Fig. 6 and TABLE 2.

TABLE 2. Comparison between old and new ETS of CSTR.

Class	Triggers	MDR
Old ETS	886	13.7%
New ETS	1003	5.1%

Remark 3: It can be seen from the Fig. 6 that faults are detected at around 340s in FD with old ETS, while are detected at around 250s in the new one, which reveals that new ETS detects faults earlier, and reduce the MDR.



*Remark 4:* Unsuitable triggering parameter of ETS in existing literature such as [19], [35] will lead to some consequences, a larger parameter will cause the loss of important information, while an ETS with small parameter cannot alleviate the network congestion. The proposed ETS has one more step than the old ETS in terms of detection data, which can save the significant information as much as possible while reducing the network congestion, and improve the detection accuracy obviously in FD.

## V. CONCLUSION

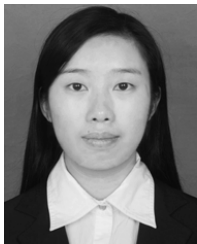
This paper develops an optimal FD approach for discrete NCSs with a new ETS. The occurrence of events are determined by a set of conditions rather than a single condition, and values in these conditions are not only the last transmitted data, but also the data within a specified time period. The FDI detects faults more precisely, and shows robustness to disturbances, where the transmission errors are also taken into account. Optimal observer gains are acquired by using the DTRE, and the time-varying thresholds are obtained by utilizing the LMI. It turns out that the approach proposed in this work can effectively reduce the MDR, and improve the detection accuracy by implementing two simulations.

It should be noted that the paper leaves some open questions, issues of NCSs such as packet loss, quantization are not taken into consideration. These issues can be further considered to improve the FD performance, such as developing relevant methods with ETS to realize the low MDR and low communication cost, these are also the topics in our further research.

## REFERENCES

- [1] X. Ge, F. Yang, and Q.-L. Han, "Distributed networked control systems: A brief overview," *Inf. Sci.*, vol. 380, pp. 117–131, Feb. 2017.
- [2] X.-M. Zhang, Q.-L. Han, and X. Yu, "Survey on recent advances in networked control systems," *IEEE Trans. Ind. Informat.*, vol. 12, no. 5, pp. 1740–1752, Oct. 2016.
- [3] B.-L. Zhang, Q.-L. Han, and X.-M. Zhang, "Event-triggered  $H_\infty$  reliable control for offshore structures in network environments," *J. Sound Vib.*, vol. 368, pp. 1–21, Apr. 2016.
- [4] A. Cuenca, D. J. Antunes, A. Castillo, P. García, B. A. Khashoeei, and W. P. M. H. Heemels, "Periodic event-triggered sampling and dual-rate control for a wireless networked control system with applications to UAVs," *IEEE Trans. Ind. Electron.*, vol. 66, no. 4, pp. 3157–3166, Apr. 2019.
- [5] C. Peng, S. Ma, and X. Xie, "Observer-based non-PDC control for networked T-S fuzzy systems with an event-triggered communication," *IEEE Trans. Cybern.*, vol. 47, no. 8, pp. 2279–2287, Aug. 2017.
- [6] J. Qiu, H. Gao, and S. X. Ding, "Recent advances on fuzzy-model-based nonlinear networked control systems: A survey," *IEEE Trans. Ind. Electron.*, vol. 63, no. 2, pp. 1207–1217, Feb. 2016.
- [7] X. Ge, Q.-L. Han, and Z. Wang, "A dynamic event-triggered transmission scheme for distributed set-membership estimation over wireless sensor networks," *IEEE Trans. Cybern.*, vol. 49, no. 1, pp. 171–183, Jan. 2019.
- [8] R. R. Nair, L. Behera, and S. Kumar, "Event-triggered finite-time integral sliding mode controller for consensus-based formation of multirobot systems with disturbances," *IEEE Trans. Control Syst. Technol.*, vol. 27, no. 1, pp. 39–47, Jan. 2019.
- [9] Y. Zhang, Y. Fan, Y. Yang, and J. Chen, "Multi-agent tracking control with dynamic leader based on event-triggered control," in *Proc. 37th Chin. Control Conf.*, Jul. 2018, pp. 6628–6632.
- [10] C. Peng and F. Li, "A survey on recent advances in event-triggered communication and control," *Inf. Sci.*, vols. 457–458, pp. 113–125, Aug. 2018.
- [11] D. P. Borgers and W. P. M. H. Heemels, "Event-separation properties of event-triggered control systems," *IEEE Trans. Autom. Control*, vol. 59, no. 10, pp. 2644–2656, Oct. 2014.
- [12] V. S. Dolk, D. P. Borgers, and W. P. M. H. Heemels, "Output-based and decentralized dynamic event-triggered control with guaranteed  $\mathcal{L}_p$ -gain performance and zero-freeness," *IEEE Trans. Autom. Control*, vol. 62, no. 1, pp. 34–49, Jan. 2017.
- [13] Y. Wang, Z. Jia, and Z. Zuo, "Dynamic event-triggered and self-triggered output feedback control of networked switched linear systems," *Neurocomputing*, vol. 314, pp. 39–47, Nov. 2018.
- [14] P. Chen and Q. L. Han, "On designing a novel self-triggered sampling scheme for networked control systems with data losses and communication delays," *IEEE Trans. Ind. Electron.*, vol. 63, no. 2, pp. 1239–1248, Feb. 2016.
- [15] F. D. Brunner, W. P. M. H. Heemels, and F. Allgöwer, "Event-triggered and self-triggered control for linear systems based on reachable sets," *Automatica*, vol. 101, pp. 15–26, Mar. 2019.
- [16] X. Ge, Q.-L. Han, and F. Yang, "Event-based set-membership leader-following consensus of networked multi-agent systems subject to limited communication resources and unknown-but-bounded noise," *IEEE Trans. Ind. Electron.*, vol. 64, no. 6, pp. 5045–5054, Jun. 2017.
- [17] Z.-G. Wu, Y. Xu, Y.-J. Pan, H. Su, and Y. Tang, "Event-triggered control for consensus problem in multi-agent systems with quantized relative state measurements and external disturbance," *IEEE Trans. Circuits Syst. I, Reg. Papers*, vol. 65, no. 7, pp. 2232–2242, Jul. 2018.
- [18] Z.-G. Wu, Y. Xu, Y.-J. Pan, P. Shi, and Q. Wang, "Event-triggered pinning control for consensus of multiagent systems with quantized information," *IEEE Trans. Syst., Man, Cybern., Syst.*, vol. 48, no. 11, pp. 1929–1938, Dec. 2017.
- [19] X. Wang and M. Lemmon, "Technical communique: On event design in event-triggered feedback systems," *Automatica*, vol. 47, no. 10, pp. 2319–2322, Oct. 2011.
- [20] G.-T. Ran, Z.-D. Lu, F.-X. Xu, and J.-X. Lu, "Event-triggered dynamic output feedback control for networked T-S fuzzy systems with asynchronous premise variables," *IEEE Access*, vol. 6, pp. 78740–78750, 2018. doi: 10.1109/ACCESS.2018.2885212.
- [21] J. Liu, Y. Zhang, Y. Yu, and C. Sun, "Fixed-time event-triggered consensus for nonlinear multiagent systems without continuous communications," *IEEE Trans. Syst., Man, Cybern., Syst.*, to be published. doi: 10.1109/TSMC.2018.2876334.
- [22] Z. Gu, P. Shi, D. Yue, and Z. Ding, "Decentralized adaptive event-triggered  $H_\infty$  filtering for a class of networked nonlinear interconnected systems," *IEEE Trans. Cybern.*, vol. 49, no. 5, pp. 1570–1579, May 2019.
- [23] J. Zhang, C. Peng, D. Du, and M. Zheng, "Adaptive event-triggered communication scheme for networked control systems with randomly occurring nonlinearities and uncertainties," *Neurocomputing*, vol. 174, pp. 475–482, Jan. 2016.
- [24] S. Hu, Y. Zhou, X. Chen, and Y. Ma, " $H_\infty$  controller design of event-triggered networked control systems under quantization and denial-of-service attacks," in *Proc. 37th Chin. Control Conf.*, Jul. 2018, pp. 6338–6443.
- [25] Y. Su, J. Wu, C. Long, and S. Li, "Event-triggered control for networked control systems under replay attacks," in *Proc. Chin. Autom. Cong.*, Nov. 2018, pp. 2636–2641.
- [26] X. Bu, H. Dong, F. Han, and G. Li, "Event-triggered distributed filtering over sensor networks with deception attacks and partial measurements," *Int. J. Gen. Syst.*, vol. 47, no. 5, pp. 522–534, Apr. 2018.
- [27] Y. Pan and G.-H. Yang, "Event-triggered fault detection filter design for nonlinear networked systems," *IEEE Trans. Syst., Man, Cybern., Syst.*, vol. 48, no. 11, pp. 1851–1862, Nov. 2018.
- [28] B. Mu, J. Chen, Y. Shi, and Y. Chang, "Design and implementation of nonuniform sampling cooperative control on a group of two-wheeled mobile robots," *IEEE Trans. Ind. Electron.*, vol. 64, no. 6, pp. 5035–5044, Jun. 2017.
- [29] M. Davoodi, N. Meskin, and K. Khorasani, "Event-triggered multiobjective control and fault diagnosis: A unified framework," *IEEE Trans. Ind. Informat.*, vol. 13, no. 1, pp. 298–311, Feb. 2017.
- [30] H. Li, Z. Chen, L. Wu, H.-K. Lam, and H. Du, "Event-triggered fault detection of nonlinear networked systems," *IEEE Trans. Cybern.*, vol. 47, no. 4, pp. 1041–1052, Apr. 2017.
- [31] Y.-L. Wang, P. Shi, C.-C. Lim, and Y. Liu, "Event-triggered fault detection filter design for a continuous-time networked control system," *IEEE Trans. Cybern.*, vol. 46, no. 12, pp. 3414–3426, Dec. 2016.

- [32] K. Peng, M. Wang, and J. Dong, "Event-triggered fault detection framework based on subspace identification method for the networked control systems," *Neurocomputing*, vol. 239, pp. 257–267, May 2017.
- [33] M. Chadli, A. Abdo, and S. X. Ding, " $H_-/H_\infty$  fault detection filter design for discrete-time Takagi–Sugeno fuzzy system," *Automatica*, vol. 49, no. 7, pp. 1996–2005, Jul. 2013.
- [34] F. Guo, X. Ren, Z. Li, and C. Han, "Fault detection for linear discrete-time systems with output quantisation," *Int. J. Control*, vol. 90, no. 10, pp. 2270–2283, 2017.
- [35] A. Qiu, A. W. Al-Dabbagh, and T. Chen, "A tradeoff approach for optimal event-triggered fault detection," *IEEE Trans. Ind. Electron.*, vol. 66, no. 3, pp. 2111–2121, Mar. 2019.
- [36] S. X. Ding, *Model-Based Fault Diagnosis Techniques: Design Schemes, Algorithms, and Tools*, 2nd ed. London, U.K.: Springer-Verlag, 2013.
- [37] K. E. S. Pilario and Y. Cao, "Canonical variate dissimilarity analysis for process incipient fault detection," *IEEE Trans. Ind. Informat.*, vol. 14, no. 12, pp. 5308–5315, Dec. 2018.



**ZHEN ZHAO** received the B.S. degree from the Tianjin University of Technology and Education, in 2015. She is currently pursuing the M.S. degree in control science and engineering with Zhejiang Sci-Tech University, Hangzhou, China. Her current research interests include networked control systems, event-triggered scheme, and fault detection.



**JINFENG GAO** received the B.S. degree from the Hebei Institute of Science and Technology, in 2000, the M.S. degree from the Zhejiang University of Technology, in 2003, and the Ph.D. degree from Zhejiang University, in 2008. She is currently a Professor with Zhejiang Sci-Tech University, Hangzhou, China. Her research interests include fault detection and diagnosis, networked control, and multi-agent systems.



**CHUNPING WANG** received the B.S. degree in automation from the Hebei Institute of Science and Technology, in 2000. He is currently a Lecturer with Zhejiang Sci-Tech University, Hangzhou, China. His research interests include networked control and multi-agent systems.

...